

Dynamic State Estimation Based on Poisson Spike Trains - Towards a Theory of Optimal Encoding

Alex Susemihl^{1,2}, Ron Meir³ and Manfred Opper^{1,2}

¹ Department of Artificial Intelligence, Technische Universität Berlin, Franklinstr. 28-29, Berlin 10587, Germany

² Bernstein Center for Computational Neuroscience Berlin, Philippstr. 13, Haus 6, Berlin 10115, Germany

³ Faculty of Electrical Engineering, Technion, Haifa 32000, Israel

Abstract. Neurons in the nervous system convey information to higher brain regions by the generation of spike trains. An important question in the field of computational neuroscience is how these sensory neurons encode environmental information in a way which may be simply analyzed by subsequent systems. Many aspects of the form and function of the nervous system have been understood using the concepts of optimal population coding. Most studies, however, have neglected the aspect of temporal coding. Here we address this shortcoming through a filtering theory of inhomogeneous Poisson processes. We derive exact relations for the minimal mean squared error of the optimal Bayesian filter and by optimizing the encoder, obtain optimal codes for populations of neurons. We also show that a class of non-Markovian, smooth stimuli are amenable to the same treatment, and provide results for the filtering and prediction error which hold for a general class of stochastic processes. This sets a sound mathematical framework for a population coding theory that takes temporal aspects into account. It also formalizes a number of studies which discussed temporal aspects of coding using time-window paradigms, by stating them in terms of correlation times and firing rates. We propose that this kind of analysis allows for a systematic study of temporal coding and will bring further insights into the nature of the neural code.

PACS numbers: 87.19ls, 87.19lo, 87.19lt

Submitted to: *Journal of Statistical Mechanics: Theory and Experiment*

1. Introduction

Populations of neurons transmit information through their joint spiking activity. One of the main goals of computational neuroscience is to gain insight into the mechanisms which shape the functional activity of neurons, and to better understand and possibly decode the information encoded by neurons. In the study of optimal population codes, it is usual to start from considerations about the nature of the neural information processing and of the tasks performed by the neurons to search for the best possible coding strategies (see for example [1, 2, 3, 4]). Considering the encoding and decoding

of stimuli from the information-theoretical viewpoint, we can develop a theory for the optimal Bayesian estimator for any given task. Given a particular estimation task and a noise model, the Bayesian estimator is the best estimator for the task, minimizing a well-defined cost function (see [5]). In the broader context of Systems Theory, spike train encoding and decoding can be viewed within the context of optimal filtering based on point process observations [6].

Here we focus on a specific question: Given a stimulus ensemble and the optimal Bayesian decoder, how can we design an **encoder** to minimize the mean squared error in a stimulus reconstruction/state estimation task? That is, we would like to determine an optimal response distribution, to make the reconstruction of the stimulus easier. This has been the subject of previous investigations in a number of contexts. In [7, 2, 3] the authors sought to answer the question in the framework of static stimuli. These papers established the existence of a finite optimal tuning width for bell-shaped tuning functions. In [1] the authors study a similar problem in the context of finite-state Markov models. In the Deep Belief Network literature, the study of Autoencoders, which deal with a very similar question, has recently received a lot of attention as well [8]. We focus here on the framework proposed in [9], where a dynamic stimulus is observed through noisy spike trains and is decoded online. This falls within the general theory of Bayesian filtering of point processes [6]. So, given an ensemble of stochastic stimuli and a family of possible encoders, we seek the encoder that minimizes the mean squared error of the Bayesian decoder (filter) in a state estimation task.

We observe that the task of designing an optimal encoder-decoder pair in our setting is very different from the case often studied within Information Theory [10], where real-time constraints are absent and solutions are asymptotic in nature, being based on infinitely increasing block sizes. In the present real-time setting, we are interested in guaranteeing good real-time performance for *finite* observation times. In fact, the problem studied in this work falls into the category of a decentralized multi-agent sequential stochastic optimization problem (viewing the encoder and decoder as agents), the general solution to which is not known [11]. The approach taken here is based on selecting a decoder using optimal Bayesian decoding assuming a fixed encoder, and then optimizing the encoder itself.

A central aspect of neural coding is its speed. Neural populations typically perform computations within less than 50 milliseconds, accounting for the fast responses characteristic of animals [12, 13]. Most studies of optimal population coding, however, still resort to the paradigm of time-slots, in which a (mostly static) stimulus is presented to a network for a given time window, spikes are pooled for each neuron and a rate code is assumed [3, 4]. Here we follow a different path, focusing on the dynamical aspect of natural stimuli, and developing the optimal Bayesian filter for a dynamic state estimation problem (this has been hinted at in [9] and developed for finite-state models in [1]). In filtering theory, one tries to estimate the value of a certain function of the system's state, given noisy observations of that system's state in the past.

Drawing from the theory of stochastic dynamics, we present a model for the joint

dynamics of signal and noise, where the signal is assumed to be a diffusion process and the noise arises from the Poisson spiking of the neurons. For the subclass of linear stochastic processes, we find that the mean squared error (MSE) is equal to the average posterior variance of the filter. This can be shown to be independent of the specific signal, and we can analyze the marginal dynamics of the variance of the filter. Analyzing this marginal dynamics, we obtain results regarding the value of the mean squared error through simulations and in a mean-field approximation, which hold in the equilibrium as well as in the relaxation period. In spite of the simplifications involved, the mean-field results are shown to be in very good agreement with the the full Monte Carlo simulations of the system.

For the linear stochastic processes considered we obtain an interesting relation for the timescales involved. Specifically, we find that whenever the average interspike interval is larger than the correlation time of the observed process, the distribution of possible errors diverges around the upper bound for the error. This implies that the firing rate of the sensory neurons must exceed a threshold in order to be able to track the input properly. The threshold is defined by the statistics of the stimulus. This relation holds exactly for the class of processes considered, and is specially pronounced in the Ornstein-Uhlenbeck process, where we present a closed-form solution of the full distribution of the posterior variance. We also provide an exact analysis of the prediction error which holds for the general class of processes discussed. Furthermore, we show that for the stimuli considered there is a finite optimal tuning width for the tuning functions which minimizes the error in the reconstruction of the stimulus. The dependence of this optimal tuning width as a function of the stimulus properties is discussed in the context of an ecological theory of sensory processing [14].

Much effort has been devoted to understand how spiking neural networks can implement operations such as marginalization, optimal inference under uncertainty and others. The finding that humans and animals combine uncertain cues from separate senses near-optimally [15, 16, 17] has given a lot of traction to this line of research. We note that this paper takes a different path. We seek the encoder that saturates the limits given by the Bayesian optimal decoder. In [18], the authors have considered a similar problem, but tried to devise a spiking neural network that would optimally decode the stimulus. Similarly, in [19] a procedure based on divisive normalization was presented that performs marginalization optimally for similar problems, and was applied to a filtering problem similar to the one considered here. We, however, focus on the optimal design of an encoder given an ensemble of stimuli assuming optimal decoding and study their relation to the statistical structure of the stimulus. This has been studied before in different settings (e.g. [1, 2, 3, 20]).

We propose that the framework of Bayesian filtering is more suited to study population coding than the usual time-binning method, as it allows for a natural inclusion of the time scales of the observed process and of the internal dynamics of the neurons. We have shown that for a simple model, we find a general relation connecting the time scales of the population spiking and that of the stimulus observed with the

error of an ideal observer. This has implications for the optimal tuning width of tuning functions of neurons. We believe that different strategies for temporal coding in different sensory systems might be traced to similar arguments, as has been done in [14] for the limit of slow temporal stimulation.

The main contribution of the present paper is in providing insight, combined with closed form mathematical expressions, for the reconstruction error of stimuli encoded by biologically motivated point processes. While precise expressions can be obtained only in limiting cases, they provide an essential starting point for a theory of optimal encoding-decoding within a biologically relevant framework, and demonstrate the importance of adaptive encoding to the neural processing of dynamic stimuli. Note that even in the simple case of linear processes observed by linear systems (e.g., [21]), it is in general impossible to obtain closed form expressions for the estimation error, and one usually resorts to bounds.

1.1. Structure of the Paper

In section 2 we present the framework used. We will derive a number of results on the Minimum Mean Squared Error (MMSE) for a stimulus reconstruction task with a Gaussian process observed through Poisson spike trains. A thorough analysis is presented for both Ornstein-Uhlenbeck processes and for smoother, non-Markovian, processes. In section 3 we will discuss the application of these results to the study of optimal population codes. Namely we show the scaling of the optimal tuning width and its corresponding MMSE as a function of the correlation structure of the process and the overall firing rate. We finalize by discussing the implications of the presented framework to the field and future applications of our framework.

2. Reconstructing Dynamic Stimuli Based on Point Process Encoding

The problem of reconstructing dynamic stimuli based on noisy partial observations falls within the general field of *filtering theory* (e.g., [21]). Consider a dynamic stimulus $\mathbf{x}(t)$, $\mathbf{x} \in \mathbb{R}^n$, which is observed through a noisy set of sensors leading to output $\mathbf{y}(t)$, $\mathbf{y} \in \mathbb{R}^m$. For example, $\mathbf{x}(t)$ could represent the position and velocity of a point object, and $\mathbf{y}(t)$ could represent the firing patterns of a set of retinal cells. The objective is to construct a filter, based only on the observation process, which provides a good estimator for the unknown value of the stimulus. Formally, denoting by $\mathbf{y}([0, t])$ the set of observations from time 0 to the present time, we wish to construct an estimator $\hat{\mathbf{x}}(\mathbf{y}([0, t]))$ which is as close as possible (in some precisely defined manner) to $\mathbf{x}(t)$. A classic example of filtering is the case of a stimulus $\mathbf{x}(t)$ generated by a noisy linear dynamical system, and an observer $\mathbf{y}(t)$ which is based on a noisy linear projection of the stimulus. The classic Kalman filter (e.g., [21]) then leads to the optimal reconstruction in the MMSE sense.

For a filtering task, the use of an \mathcal{L}_p norm as a cost function is a natural choice, given that we are interested in reconstructing the system's state as precisely as possible. Here we choose to use the \mathcal{L}_2 norm as a cost function for our reconstruction task. This is a natural choice for a filtering task (see [21]) and has been frequently used in studies of optimal population coding [1, 2, 3]. Another popular cost function for studies of optimal population coding is the mutual information between the input distribution and the conditional response distribution [4]. This allows one to find the code that optimally codes the information contained in the input in its response. Though recent theoretical advances are sketching out the relationship between information- and MMSE-optimal codes [22, 23, 24], there seems to be no simple equivalence between these two cost functions. In Gaussian additive channels, the MMSE is equal to the derivative of the mutual information between input and output with respect to the signal-to-noise ratio. Though similar relationships have been derived for Poisson processes, these hold only for linearly modulated inhomogeneous processes and do not relate directly to the MMSE [24, 25]. Furthermore, these results have been derived only for single point processes, not for populations thereof. We therefore choose to work strictly with the \mathcal{L}_2 cost function, as this is not only a natural choice for the problem at hand, but also allows for a number of analytical results.

We consider the case of linear Gaussian stochastic processes observed by a population of neurons with unimodal tuning functions. This is analogous to considering stimuli drawn from a Gaussian process prior, as has been done in [9]. We will have a prior distribution over the stimulus $x(t)$ given by a Gaussian process with zero mean and covariance function $K(t, t') = \langle x(t)x(t') \rangle$, where the angled brackets denote the average over the ensemble of Gaussian processes.

Rather than considering general Gaussian processes we will focus on a class of processes which are particularly amenable to analytic investigation. This will allow us to consider both simple Markov Gaussian processes (the so-called Ornstein-Uhlenbeck process) and higher order Markov Gaussian processes. We will consider stochastic processes described by a stochastic differential equation of the form

$$\left(\frac{d}{dt} + \gamma \right)^P x(t) = \eta \frac{dW(t)}{dt}, \quad (1)$$

where $W(t)$ is a scalar Wiener process. We can find the covariance of the process by calculating the Fourier transform, computing the power spectrum and then reversing the Fourier transform. We will have

$$\langle \tilde{x}(\omega) \tilde{x}^*(\omega) \rangle = \frac{\eta^2}{(\gamma + 2\pi i \omega)^P (\gamma - 2\pi i \omega)^P}. \quad (2)$$

This power spectrum leads to stochastic processes with the so-called Matern kernel [26, p. 211]. If unobserved, the distribution over x will converge to the equilibrium distribution, given by a Gaussian distribution with zero mean and covariance $\sigma_x^2 = \eta^2 / 2^P \gamma^{2P-1}$. These processes can also be written as multidimensional first-order processes by defining $\mathbf{X}(t) \equiv (\mathbf{X}_1(t), \mathbf{X}_2(t), \dots, \mathbf{X}_P(t))^T =$

$(x(t), x^{(1)}(t), \dots, x^{(P-1)}(t))^\top$, where $x^{(i)}(t)$ denotes the i -th derivative of $x(t)$, and its associated stochastic differential equation

$$d\mathbf{X}(t) = -\Gamma\mathbf{X}(t)dt + Hd\mathbf{W}(t), \quad (3)$$

where $\mathbf{W}(t)$ is a P -dimensional Wiener process. Γ and H are defined in Appendix A. Note that the process $x(t)$ itself will not in general be Markovian. The process $\mathbf{X}(t)$ of $x(t)$ along with its first $P - 1$ derivatives will, however, be Markov. This allows us to treat smooth non-Markov dynamics as the marginal case of a higher-dimensional Markov stimulus and so to draw from the theory of Markov stochastic processes, which is very well-established [27].

The spike trains will be modeled by inhomogeneous Poisson processes $N^m(t)$, namely, Poisson processes whose rates are functions of the stochastic process $\mathbf{X}(t)$. More precisely, $N^m(t)$ represents the number of times neuron m has spiked since the beginning of the experiment. Furthermore, we will assume each spike train $N^i(t)$ to be conditionally independent of all others, that is, given a value of the stimulus $\mathbf{X}(t)$ the spiking of each neuron is independent of all others. The function relating the stimulus $\mathbf{X}(t)$ to the rate of the Poisson process is often referred to as a tuning function, and will be denoted by $\lambda_m(\mathbf{X}(t))$. We will consider unimodal tuning function of the form

$$\lambda_m(x(t)) = \phi \exp\left(-\frac{(x(t) - \theta_m)^2}{2\alpha^2}\right),$$

where θ_m is the preferred stimulus value of neuron m . Tuning functions of this form are often found in orientation-selective cells in visual cortex of mammals and in place cells in the hippocampus [28, 29, 30]. For multi-dimensional stimuli, we can write these more generally as

$$\lambda_m(\mathbf{X}(t)) = \phi \exp\left(-(\mathbf{X}(t) - \Theta_m)^\top A^+(\mathbf{X}(t) - \Theta_m)/2\right).$$

We will prefer this notation as it allows us to derive a general theory which also holds for multidimensional stimuli. The case of a one-dimensional P -th order process along with its $P - 1$ derivatives would be recovered by setting $A_{i,j}^+ = \delta_{1,i}\delta_{1,j}/\alpha^2$ and $\Theta_m = (\theta_m, 0, \dots, 0)$. While in many cases biological tuning functions are unimodal, we have chosen to work with Gaussian functions for reasons on analytic tractability.

The likelihood of a spike train $\{N^m([0, t])\}$ is given by (see [31])

$$\mathcal{L}(\{N^m([0, t])\}|\mathbf{X}([0, t])) = \exp\left(\sum_m \int dN^m(t) \log(\lambda_m(\mathbf{X}(t))) - \sum_m \int dt \lambda_m(\mathbf{X}(t))\right).$$

We have denoted here by $\{N^m([0, t])\}$ the value of all spiking processes $N^m(s)$ for any instant s such that $0 \leq s \leq t$, and likewise $\mathbf{X}([0, t])$ denotes all values of $\mathbf{X}(s)$, for all s such that $0 \leq s \leq t$. With this likelihood we can then find the posterior distribution for $\mathbf{X}([0, t])$ using Bayes' rule,

$$P(\mathbf{X}([0, t])|\{N^m([0, t])\}) \propto \mathcal{L}(\{N^m([0, t])\}|\mathbf{X}([0, t]))P(\mathbf{X}([0, t])).$$

Averaging out the values of $\mathbf{X}(t)$ up to but excluding the time t , will give us the time-dependent Gaussian posterior $P(\mathbf{X}(t)|\{N^m([0, t])\})$. If the likelihood were Gaussian in \mathbf{X} we could use results from conditional distributions on Gaussian measures to average over $\mathbf{X}([0, t])$ (for more details, see [9]). This is indeed the case when the tuning functions are densely packed, as we will see in the following.

Let us then turn to the spiking dynamics of the whole population. Because each neuron spikes as a Poisson process with rate $\lambda_m(\mathbf{X}(t))$, and the processes $N^m(t)$ are conditionally independent when conditioned on $\mathbf{X}(t)$, the process $N(t) = \sum_m N^m(t)$ is also Poisson with rate $\lambda(\mathbf{X}(t)) \equiv \sum_m \lambda_m(\mathbf{X}(t))$. If the neurons' tuning functions are dense, however, the sum does not depend on $\mathbf{X}(t)$ and therefore the overall firing rate of the population does not depend on the stimulus at all. The rate can be estimated for equally spaced tuning centers Θ_m by considering it a Riemann sum [2]. Assuming the tuning centers Θ_m are tiled in a regular lattice with spacing $\Delta\Theta$ along each axis, we have

$$\lambda = \phi \sum_m \exp(-(\Theta_m - X)^\top A^+ (\Theta_m - X)/2) \approx \frac{\phi [(2\pi)^{\text{rank}(A)} \det^*(A)]^{1/2}}{|\Delta\Theta|^n},$$

where $\det^*(A)$ is the pseudo-determinant of A defined in Appendix B. The assumption of dense tuning functions is clearly very strong as the number of neurons necessary to cover an n -dimensional stimulus space grows exponentially with n . Note however, that the deviation from this approximation is very small when the tuning center spacing is of the order of the diagonal elements of A , i.e. when the tuning functions have a strong overlap. If this assumption is violated we would have to treat the filtering problem through the stochastic partial differential equation for the probability, as was done in [6] for general Poisson processes.

Given the assumption of dense tuning functions and due to the prior assumption about $x(t)$, the likelihood becomes Gaussian, and the posterior distribution $P(\mathbf{X}(t)|\{N^m([0, t])\})$ will also be Gaussian. Since the dynamics of $\mathbf{X}(t)$ is linear, the Gaussian distribution will be conserved and, in the absence of spikes, the mean $\mu(t)$ and covariance $\Sigma(t) = \langle (\mathbf{X}(t) - \mu(t))(\mathbf{X}(t) - \mu(t))^\top \rangle$ will evolve as

$$\frac{d\mu(t)}{dt} = -\Gamma\mu(t), \tag{4a}$$

and

$$\frac{d\Sigma(t)}{dt} = -\Gamma\Sigma(t) - \Sigma(t)\Gamma^\top + H^2. \tag{4b}$$

If a spike from a neuron m occurs at a time t , the posterior distribution of $\mathbf{X}(t)$ gets updated via Bayes' rule. The prior is then given by $\mathcal{N}(\mathbf{X}(t); \mu(t), \Sigma(t))$ and the likelihood is $\mathcal{N}(\mathbf{X}(t); \Theta_m, A)$. We denote the mean and covariance immediately after the spike at time t by $\mu(t^+)$ and $\Sigma(t^+)$. By standard Gaussian properties we obtain

$$\begin{aligned} \mu(t^+) &= (\Sigma(t)^{-1} + A^+)^{-1} (\Sigma(t)^{-1}\mu(t) + A^+\Theta_m) \\ &= \mu(t) + (\Sigma(t)^{-1} + A^+)^{-1} A^+ (\Theta_m - \mu(t)) \end{aligned} \tag{5a}$$

$$\begin{aligned}\Sigma(t^+) &= (\Sigma(t)^{-1} + A^+)^{-1} \\ &= \Sigma(t) + (\Sigma(t)^{-1} + A^+)^{-1} A^+ \Sigma(t)\end{aligned}\tag{5b}$$

This fully determines the optimal Bayesian filter, namely, it is given by $P_t(\mathbf{X}) = \mathcal{N}(\mathbf{X}; \mu(t), \Sigma(t))$, where the evolution of $\mu(t)$ and $\Sigma(t)$ is given by (4a) and (4b) in the absence of spikes and by (5a) and (5b) whenever there are spikes. It is interesting to observe that the dynamics of the mean and variance between spikes, given in (4a) and (4b), is precisely that obtained for the continuous time Kalman filter [21] when observations are absent. This is not surprising since between spikes we are tracking a linear dynamical system, as does the Kalman filter.

In order to determine the properties of the optimal encoder, we aim at obtaining expressions for the mean-squared error of the optimal filter. This gives us a measure of the best-case performance that can be achieved for a signal reconstruction task from the observation of the spike train. Specifically, we want a measure of the average performance over all stimuli and all spike trains. For that, note that because of the Gaussian nature of the stimulus and the linear dynamics of the prior, the evolution of the posterior variance does not depend on the spike trains of each neuron, but rather only on $N(t)$, the total spike count of the population. The average of the posterior covariance matrix is given by

$$\mathcal{S}(t) = \langle (\mathbf{X}(t) - \mu(t))(\mathbf{X}(t) - \mu(t))^{\top} \rangle_{\mathbf{X}, \{N^m([0, t])\}}.$$

Note that the diagonal terms give us the mean squared error on the estimation of every coordinate of $\mathbf{X}(t)$. More specifically, the MMSE in the estimation of $x(t)$ is given by $\mathcal{S}_{11}(t)$. We can simplify this by noting that $\mu(t) = \mathbf{E}(\mathbf{X}(t) | \{N^m([0, t])\})$ and evaluating the average over $P(\mathbf{X}(t) | \{N^m([0, t])\})$ [2]. We have

$$\mathcal{S}(t) = \langle \Sigma(t) \rangle_{\{N^m([0, t])\}} = \langle \Sigma(t) \rangle_{N([0, t])},$$

where in the last step we have used the fact that the dynamics of $\Sigma(t)$, and therefore its average, only depend on the population spike count $N(t)$. Up to the last step, this derivation is generally valid, though one must take care to consider the marginal distribution of the observations, averaging out the signal. Note that, although we can give an account of the temporal evolution of the mean squared error this cannot be given a biological interpretation in the absence of an experiment to contextualize the time dependence of the error. However, in the limit of long spike trains, the MSE will converge to its equilibrium value (see figure 1 and figure 3) and we can study the equilibrium statistics of $\Sigma(t)$ to determine the average MSE of the reconstruction task.

We will look at the transition probability for $\Sigma(t)$ after marginalization over $N(t)$. Consider the probability $P(\Sigma', t + dt | \Sigma, t)$, of the covariance having a value Σ' at time $t + dt$ given that at time t the covariance was Σ . For infinitesimal dt , Σ' is either given by (4b), or with a probability λdt there is a jump as specified in (5b), with $\lambda = \sum_m \lambda_m$. This will yield the transition probability

$$\begin{aligned}P(\Sigma', t + dt | \Sigma, t) &= (1 - \lambda dt) \delta(\Sigma' - \Sigma - dt(H^2 - \Gamma\Sigma - \Sigma\Gamma^T)) \\ &\quad + \lambda dt \delta(\Sigma' - (\Sigma^{-1} + A^+)^{-1}).\end{aligned}\tag{6}$$

The evolution of the time-dependent probability over the covariance matrices $P(\Sigma, t)$ will be given by the Chapman-Kolmogorov equation [27, p.47]

$$\frac{\partial P(\Sigma, t)}{\partial t} = -\nabla [B(\Sigma)P(\Sigma, t)] + \lambda C(\Sigma)P((\Sigma^{-1} - A^+)^{-1}, t) - \lambda P(\Sigma, t), \quad (7)$$

where $B(\Sigma) = -\Gamma\Sigma - \Sigma\Gamma^\top + H^2$. Note that this gives us the $MSE(t)$ through the average of Σ over the distribution $P(\Sigma, t)$. The term $C(\Sigma)$ arises from the integration of the second Dirac delta function in (6) and is given by $C(\Sigma) = 1/|\det(J(\Sigma))|$, where $J(\Sigma)$ is the Jacobian matrix

$$J_{(i,j),(k,l)} = \frac{\partial(\Sigma^{-1} + A^+)_{i,j}^{-1}}{\partial \Sigma_{k,l}} = (I + A^+\Sigma)_{k,i}^{-1}(I + \Sigma A^+)_{j,n}^{-1}$$

The exact choice of the ordering of the indices is not of importance, as it would only account for a change in the sign of the determinant in $C(\Sigma)$, which only enters the equation through its absolute value. This term is not of great importance, however, as it will be cancelled when we calculate the evolution of the averages.

We can now formalize what we mean by the equilibrium condition mentioned above. Note that under the stimulus and noise models proposed the evolution of the distribution of the error is given by (7). Given some initial condition for $P(\Sigma, t_0)$, the distribution will evolve and eventually it will reach an equilibrium, such that $\partial_t P(\Sigma, t) = 0$. We are interested in this equilibrium regime, as it provides the average performance of the optimal filter after all transients from the initial conditions have vanished.

The evolution of $\mathcal{S}(t) = \langle \Sigma \rangle_t$ can be found easily from (7). Using

$$\frac{d}{dt} \int d\Sigma f(\Sigma) P(\Sigma, t) = \int d\Sigma f(\Sigma) \frac{\partial P(\Sigma, t)}{\partial t},$$

and integrating by parts we obtain

$$\frac{d \langle \Sigma \rangle_t}{dt} = -\Gamma \langle \Sigma \rangle_t - \langle \Sigma \rangle_t \Gamma^\top + H^2 + \lambda \left\langle (\Sigma^{-1} + A^+)^{-1} A^+ \Sigma \right\rangle_t, \quad (8)$$

where $\langle f(\Sigma) \rangle_t = \int d\Sigma f(\Sigma) P(\Sigma, t)$. This cannot be treated exactly, though, as the nonlinear averages on the right hand side are intractable even for simple cases. Similar relations for the evolution of the average mean and variance of a filter were presented in [6] as approximations to the true filter (based on discarding higher order moments).

The evolution of the distribution over covariance matrices is thus determined. However, evaluating the averages is intractable even for the case of dense neurons when λ is independent of $\mathbf{X}(t)$. We will therefore look into three different ways of treating (7). First, we can simply simulate the population spiking process $N(t)$ as a Poisson process to obtain samples of $P(\Sigma, t)$. By averaging over multiple realizations of $N(t)$ we can estimate the average value of $\Sigma(t)$ and by monitoring its evolution we can determine when it has relaxed to the equilibrium. The second possibility is to analyze (8) in a mean-field approximation, i.e. to simply replace all averages of the form $\langle f(\Sigma) \rangle$

with $f(\langle \Sigma \rangle)$, disregarding all fluctuations around the mean. We would then have the dynamics

$$\frac{d\langle \Sigma \rangle_t}{dt} = -\Gamma \langle \Sigma \rangle_t - \langle \Sigma \rangle_t \Gamma^\top + H^2 + \lambda (\langle \Sigma(t) \rangle_t^{-1} + A^+)^{-1} A^+ \langle \Sigma(t) \rangle_t. \quad (9)$$

A third possibility is to analyze (7) directly. This leads to a number of interesting results for the one-dimensional Ornstein-Uhlenbeck process, but the generalization to higher dimensions is not straightforward. We will proceed by analyzing the case of the Ornstein-Uhlenbeck process first. Subsequently we will look at the case of smoother linear stochastic processes, which are produced by Gaussian processes with Matern kernels [26]. The generalization to linear diffusion processes is straightforward. We will finalize this section with a discussion of the prediction error for the optimal filter considered.

2.1. Filtering the Ornstein-Uhlenbeck Process

As is well known, the OU process is the only homogeneous Markov Gaussian process in one dimension, and is therefore particularly convenient as a starting point for analysis [27]. When we consider the OU process described by the stochastic differential equation

$$dx(t) = -\gamma x(t)dt + \eta dW(t),$$

the analysis we presented above is greatly simplified. The evolution of the posterior variance s is then given simply by

$$\frac{d\langle s \rangle_t}{dt} = -2\gamma \langle s \rangle_t + \eta^2 - \lambda \left\langle \frac{s^2}{\alpha^2 + s} \right\rangle_t. \quad (10)$$

We will denote the one-dimensional variance by s , reserving Σ for the multidimensional covariance matrix. In the case of the OU process we can give a more complete account of the distribution of the errors for the filter. For the one-dimensional case (7) simplifies to

$$\frac{\partial P(s, t)}{\partial t} = \frac{\partial}{\partial s} [(2\gamma s - \eta^2)P(s, t)] + \lambda \left(\frac{\alpha^2}{\alpha^2 - s} \right)^2 P\left(\frac{\alpha^2 s}{\alpha^2 - s}, t \right) - \lambda P(s, t). \quad (11)$$

Clearly $P(s, t) = 0, \forall s < 0$. In the equilibrium we will have

$$-\frac{d}{ds} [(2\gamma s - \eta^2)P(s)] = \lambda \left(\frac{\alpha^2}{\alpha^2 - s} \right)^2 P\left(\frac{\alpha^2 s}{\alpha^2 - s} \right) - \lambda P(s). \quad (12)$$

This is a delayed-differential equation with nonlinear delays in s . [To see this, note that for every \$s\$ such that \$0 < s < \alpha^2\$, we have \$\alpha^2 s / \(\alpha^2 - s\) > s\$. For \$s > \alpha^2\$, this term becomes meaningless, as the posterior variance will always fall below \$\alpha^2\$ after the observation of a spike.](#) This means, that for any $s > 0$, the derivative of $P(s)$ is a function of $P(s)$ and $P(\alpha^2 s / (\alpha^2 - s))$. Defining the function $j(s) = \alpha^2 s / (\alpha^2 - s)$ we can define intervals $I_0 = [j(s_0), s_0]$, $I_1 = [j^2(s_0), j(s_0)]$, ... with $s_0 = \eta^2 / 2\gamma$. We will then have that given the solution of $P(s)$ on I_n , the solution in I_{n+1} is the solution of a simple inhomogeneous ordinary differential equation with a continuity condition

on $j^n(s_0)$. This can be simply solved through numerical integration schemes. We will show in Appendix C that in the equilibrium $P(s > \eta^2/2\gamma) = 0$. We therefore define the boundary conditions as $P_{eq}(s) = 0, \forall s > \eta^2/2\gamma$. This will imply that the jump term in (12) will be absent whenever the jump originates in the domain $s > \eta^2/2\gamma$. This is the case when $s \in I_0$. For these values of s we arrive at

$$\frac{d}{ds} [(2\gamma s - \eta^2)P_{eq}(s)] - \lambda P_{eq}(s) = 0. \quad (13)$$

This is solved by

$$P_{eq}(s) = C \left(\frac{\eta^2}{2\gamma} - s \right)^{\frac{\lambda}{2\gamma} - 1}, \quad s \in I_0. \quad (14)$$

We can use this solution as a boundary condition to solve (12) as a delayed-differential equation with variable delays, but an analytical solution is not available for the subsequent intervals. In figure 2 we present the numerical solution of (12) alongside with histograms from simulations. Note that the solution in (14) is exact for the interval I_0 and is therefore in significant agreement with the simulations. In the subsequent intervals numerical errors degrade the precision of the solution. Especially when α is very large the intervals I_n will get smaller, and the numerical integration of (12) will become less stable.

This solution can also be obtained in the limit of very small firing rates, that is when $\lambda \ll 2\gamma$. We can then assume that between two spikes the variance has already relaxed to its free equilibrium value s_0 . A spike at time t_s will then take the variance to $s' = j(s_0)$. The evolution will then be given by

$$s(t) = e^{-2\gamma(t-t_s)} s' + s_0(1 - e^{-2\gamma(t-t_s)}),$$

which can be inverted into

$$t - t_s = -\frac{1}{2\gamma} \log \left(\frac{s_0 - s(t)}{s_0 - s'} \right).$$

We can then write the distribution over s as a distribution over interspike intervals $\tau = t - t_s$. We know the probability distribution over τ is given by an exponential with coefficient λ . Changing the variables, we will have

$$P(s) = P(\tau) \left| \frac{d\tau}{ds} \right| \propto e^{-\lambda\tau} e^{2\gamma\tau}.$$

Which in turn gives us (14) for the equilibrium distribution of s . Note that this derivation only holds in the limit of $\lambda \ll 2\gamma$, while the deduction above for the interval $[s', s_0)$ holds irregardless of the value of the parameters. The mentioned limit is very useful in the multidimensional case, however.

In the mean-field approximation for the equilibrium condition we will have

$$\frac{ds}{dt} = -2\gamma s + \eta^2 - \lambda \frac{s^2}{\alpha^2 + s}. \quad (15)$$

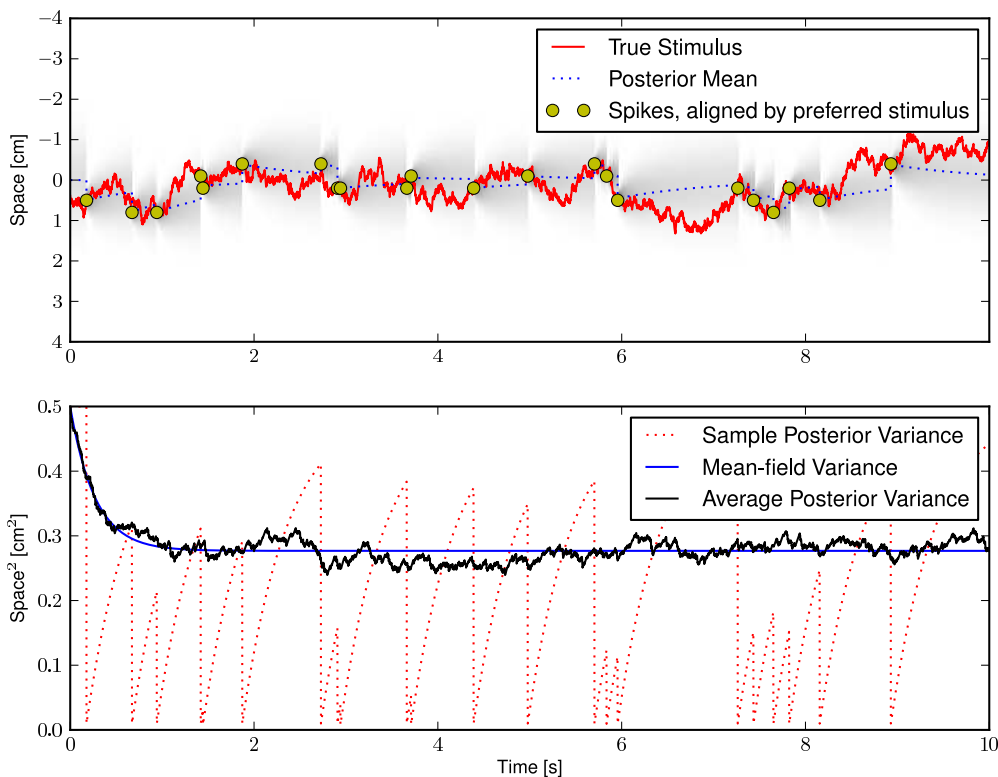


Figure 1: General setup of the inference task. The upper panel shows the true stimulus or signal $x(t)$ in red solid line, the filtered posterior mean in the blue dotted line and the shading represents the posterior probability distribution. The lower panel shows the evolution of the posterior variance. The red dotted line gives the sample variance of the sample in the upper panel, the solid black line shows an average over 100 realizations and the blue line gives the evolution of the mean-field equation with the same initial conditions.

This gives a remarkably good account of the equilibrium properties of the system, as is shown in figure 1. Surprisingly, the mean-field equation gives a very good account of the transient behavior of the error as well as of the equilibrium.

We can also derive a simple Gaussian approximation for the rescaled inverse variance $z = \eta^2/(\gamma s)$. Note that the distribution of the inverse variance at the equilibrium is given by

$$-\frac{d}{dz} [\gamma z(2-z)P_{eq}(z)] + \lambda P_{eq}(z - \frac{\eta^2}{\gamma \alpha^2}) - \lambda P_{eq}(z) = 0. \quad (16)$$

In the limit where $\eta^2/\gamma \alpha^2 \ll z$ we can Taylor expand the second term to second order. In this regime we will have very broad tuning functions and each individual spike will have little effect. This can be thought of as a diffusion limit. Further linearizing the drift term around its equilibrium we will obtain the Van Kampen expansion for

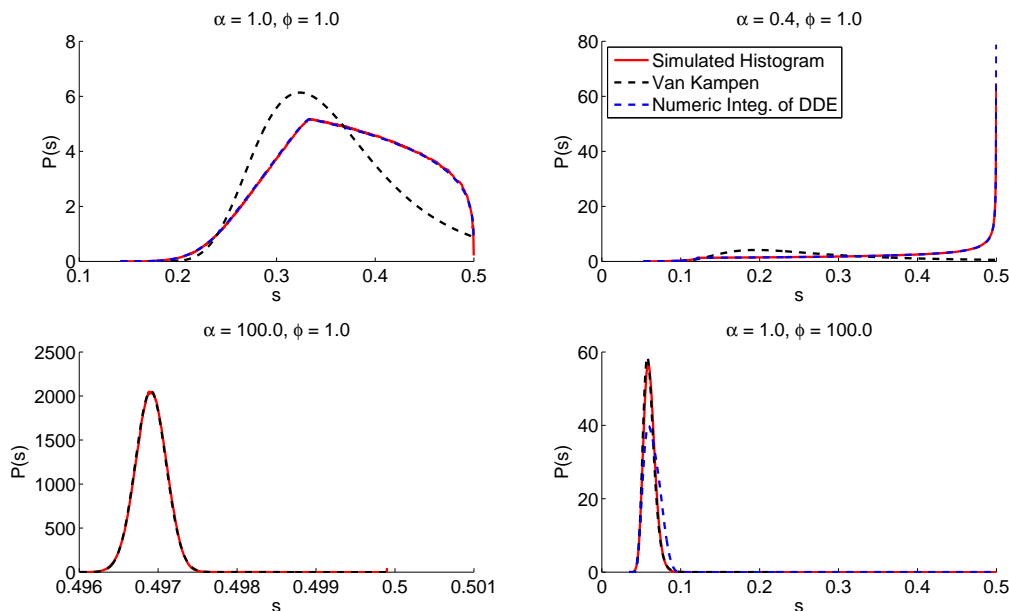


Figure 2: Different treatments of the distribution of the variance for different sets of parameters of the encoder for a first-order OU stimulus. The red line shows the histogram obtained through simulations. The blue line shows the numerical integration of (12) using the mentioned boundary condition. The black line shows the Van Kampen expansion given in the text. Note that the numerical integration of (12) provides a very good account of the simulated histogram, except for very large values of α , when the integration becomes unstable. The Van Kampen approximation in turn provides a good account for the limit of large firing rates, for large α as well as for large ϕ .

the problem [27]. It will lead to a Fokker-Planck equation whose solution is the Gaussian distribution $P_z(z) = \mathcal{N}\left(1 + [1 + \lambda\delta/\gamma]^{1/2}, \lambda\delta^2 [4\gamma]^{-1} [1 + \lambda\delta/\gamma]^{-1/2}\right)$. By writing $P(s) = P_z(\eta^2/\gamma s)\eta^2/\gamma s^2$ we can then recover the distribution over the variances. These results are all compared in figure 2.

2.2. Filtering Smooth Processes

In section 2.1 we considered Markovian Gaussian processes. However, within an ecologically oriented setting, it is often more natural to assume smooth priors [9]. Since in general smooth priors lead to non-Markovian processes, which are very hard to deal with mathematically, we look at a special case of a smooth non-Markovian prior. Specifically, we will look at the multidimensional embedding $\mathbf{X}(t)$ of the smooth processes given by (3). We choose to study these processes as they allow us to consider smooth stochastic processes with the same set of parameters as were used to consider the OU process. Figure 3 shows the general inference framework for higher-order smooth processes.

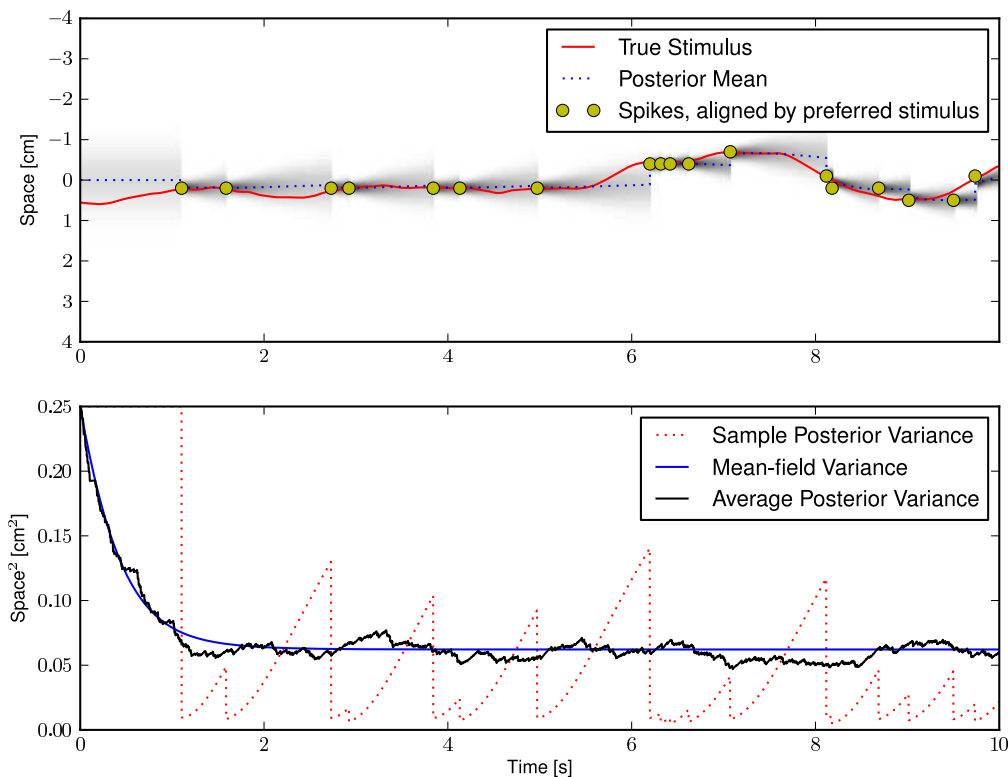


Figure 3: Inference task for the $P = 2$ process. The upper panel shows the true stimulus or signal $x(t)$ in red solid line, the filtered posterior mean in the blue dotted line and the shading represents the posterior probability distribution. The lower panel shows the evolution of the posterior variance. The red dotted line gives the sample variance of the sample in the upper panel, the solid black line shows an average over 100 realizations and the blue line gives the evolution of the mean-field equation with the same initial conditions.

Taking the observation matrix $A_{ij} = \delta_{1,i}\delta_{1,j}\alpha^2$ with pseudo-inverse $A^+ = \delta_{1,i}\delta_{1,j}/\alpha^2$, the form of A will allow us to somewhat simplify equation (5b) and we can write a simple mean-field equation for the evolution of $\langle \Sigma \rangle_t = \bar{\Sigma}(t)$. We have in the mean-field approximation

$$\frac{d\bar{\Sigma}(t)}{dt} = -\Gamma\bar{\Sigma}(t) - \bar{\Sigma}(t)\Gamma^\top + H^2 - \lambda \frac{\bar{\Sigma}(t)A^+\bar{\Sigma}(t)}{1 + \bar{\Sigma}(t)_{1,1}/\alpha^2}. \quad (17)$$

This equation still describes the average performance of the Bayesian filter remarkably well, not only in the equilibrium phase but also in the transient period (see figure 3). Note that the sole contributor to the nonlinearity in the equation above is the first column of the covariance matrix. Given $\bar{\Sigma}_{1,j}$ solving for the remaining elements of the matrix is a matter of linear algebra.

The argument made in Appendix C cannot be rigorously be made here, as we have

Σ evolving in a high dimensional space with nonlinear jumps. In principle, one could map out a subspace such that $P(\Sigma, t)$ is zero outside of it, and then proceed to locate a set of Σ such that $(\Sigma^{-1} - A^+)^{-1}$ falls in it, and then seek to solve equation (7) in that domain. This could, in principle, be made rigorous, but as we will see below, this approach is not as useful when considering smoother processes. To see why, let us study the small λ limit as we did in the OU process. Assuming $\lambda \ll \nabla \cdot B$, we can assume that the covariance matrix has nearly relaxed to its equilibrium value Σ_0 every time there is a spike. Whenever there is a spike the covariance matrix jumps to $\Sigma' = (\Sigma_0^{-1} + A^+)^{-1}$. The free evolution is then given by

$$\Sigma(t) = e^{-(t-t_0)\Gamma} \Sigma' e^{-(t-t_0)\Gamma^\top} + \int_{t_0}^t ds e^{-(t-s)\Gamma} H^2 e^{-(t-s)\Gamma^\top}.$$

Changing variables to $\tau = t - t_0$ we have

$$\Sigma(\tau) = e^{-\tau\Gamma} \Sigma' e^{-\tau\Gamma^\top} + \int_0^\tau ds e^{-s\Gamma} H^2 e^{-s\Gamma^\top}.$$

Clearly there is no simple solution to these matrix equations as there is for the OU case, but we can still use the same approach as before numerically. We can assume an unknown function of Σ that gives us the time since the spike $\tau(\Sigma)$. We can then proceed as before and evaluate the marginal distributions. We would have for $\Sigma_{1,1}$

$$P(\Sigma_{11}) = \frac{P(\tau(\Sigma_{11}))}{\left| \frac{d\Sigma_{11}}{d\tau} \right|} \propto \frac{e^{-\lambda\tau}}{\left| \frac{d\Sigma_{11}}{d\tau} \right|}.$$

When we analyzed the analog of this relation for the OU process we could find a simple correspondence between the divergence of the distribution around the equilibrium value of the variance and the parameters λ and γ . Though we can argue similarly in this case, note that immediately after the jump, we have $d\Sigma_{11}/d\tau = \Sigma'_{12} = 0$ which results itself in a divergence in the distribution in this approximation. So, even in the limit $\lambda \ll \nabla \cdot B$, there is always some probability mass concentrated around the value Σ' , so the divergence argument is not so strong for smoother processes. This can be seen in figure 4.

2.3. Prediction Error

The prediction error can easily be derived as a function of the filtering error in this framework. We have the predictive probability $P(\mathbf{X}_{t+\delta} | \{N^m([0, t])\})$, with $\delta > 0$. The average prediction error would simply be the deviation of $\mathbf{X}_{t+\delta}$ from the estimator $\mu(t + \delta)$. The prediction error is then

$$\mathcal{P}(\delta) = \left\langle (\mathbf{X}(t + \delta) - \mu(t + \delta)) (\mathbf{X}(t + \delta) - \mu(t + \delta))^\top \right\rangle_{\mathbf{X}, \{N^m([0, t])\}}. \quad (18)$$

This gives us the matrix $\mathcal{S}(t)$ when $\delta = 0$. For $\delta > 0$ we have the prediction error matrix. Note that given a value of $\mathbf{X}(t)$ and a realization of the Wiener process $d\mathbf{W}(s)$ for $t \leq s \leq t + \delta$, we have $\mathbf{X}(t + \delta) = \int_t^{t+\delta} e^{-(t+\delta-s)\Gamma} H d\mathbf{W}(s) + e^{-\delta\Gamma} \mathbf{X}(t)$. Clearly,

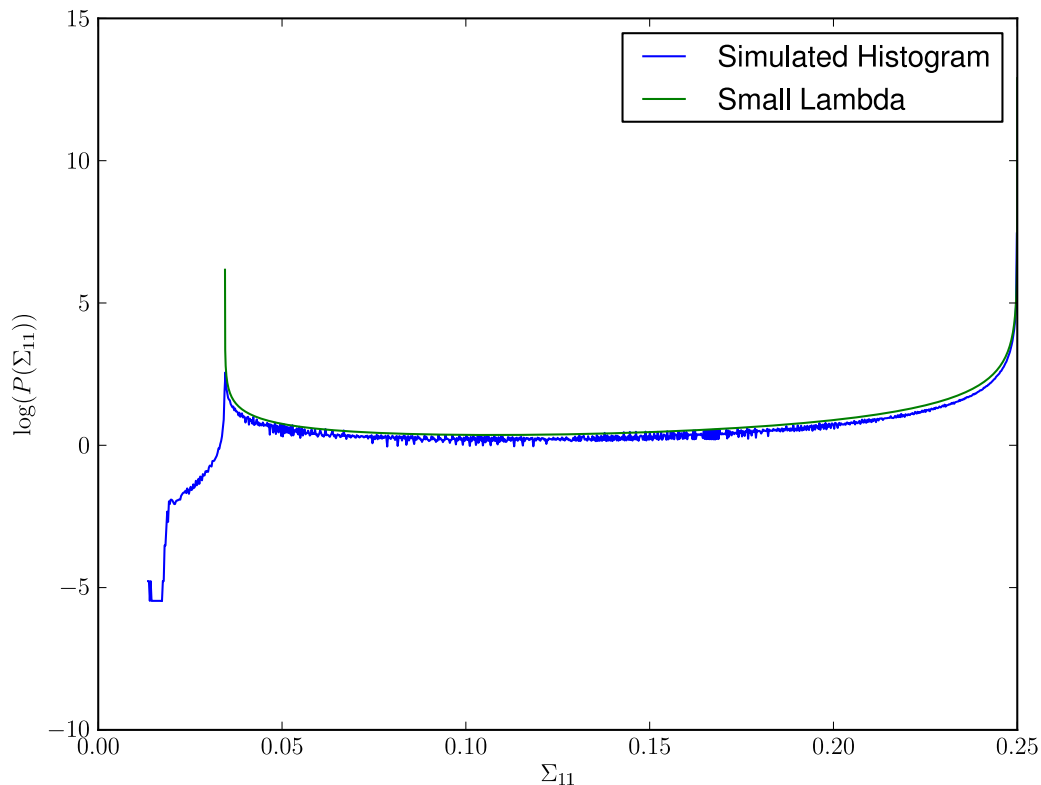


Figure 4: The small firing rate approximation provides a very good account of the distribution of the variance of the observed process Σ_{11} .

conditioning on $\mathbf{X}(t)$ the above average is only over the Wiener process between t and $t + \delta$. The estimator $\mu(t + \delta)$ is also given by $\mu(t + \delta) = e^{-\delta\Gamma}\mu(t)$ in the absence of spikes. The prediction error matrix will then be given by

$$\mathcal{P}(\delta) = \left\langle \left(\int_t^{t+\delta} e^{-(t+\delta-s)\Gamma} H d\mathbf{W}(s) + e^{-\delta\Gamma} \mathbf{X}(t) - e^{-\delta\Gamma} \mu(t) \right) \times \left(\int_t^{t+\delta} e^{-(t+\delta-u)\Gamma} H d\mathbf{W}(u) + e^{-\delta\Gamma} \mathbf{X}(t) - e^{-\delta\Gamma} \mu(t) \right)^\top \right\rangle_{\mathbf{X}, \{N^m([0,t])\}} \quad (19)$$

Since $e^{-(t+\delta-u)\Gamma} H$ is non-anticipating and does not depend on $\mathbf{X}(t)$ or $N^m(t)$, we have that (see [27])

$$\left\langle \int_t^{t+\delta} e^{-(t+\delta-u)\Gamma} H d\mathbf{W}(u) \int_t^{t+\delta} (e^{-(t+\delta-s)\Gamma} H d\mathbf{W}(s))^\top \right\rangle = \int_t^{t+\delta} e^{-(t+\delta-u)\Gamma} H^2 e^{-(t+\delta-u)\Gamma^\top} du$$

and therefore, changing variables,

$$\mathcal{P}(\delta) = e^{-\delta\Gamma} \mathcal{P}(0) e^{-\delta\Gamma^\top} + \int_0^\delta e^{-s\Gamma} H^2 e^{-s\Gamma^\top} ds. \quad (20)$$

This is the usual relation for the evolution of the variance of linear stochastic processes, and it shows us that the prediction error is a simple function of the filtering error. This

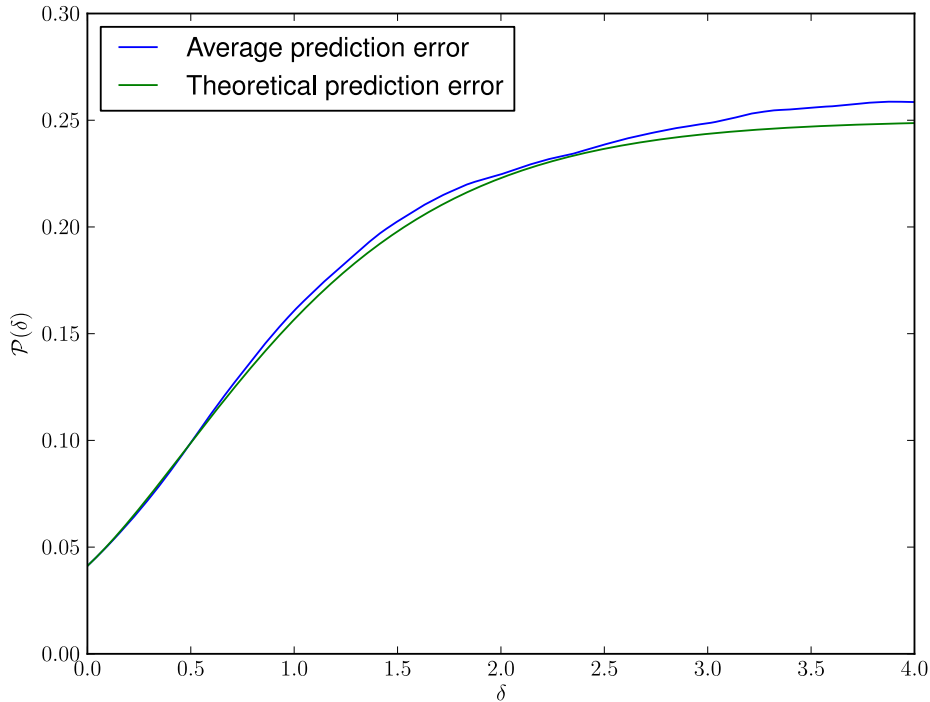


Figure 5: The evolution of the average prediction error $\mathcal{P}(\delta)$ is completely determined by the filtering error $\mathcal{P}(0)$. The blue line shows the prediction error obtained from the optimal filter in simulations, whereas the green line shows the evolution of the prediction error according to (20) with the initial condition given by the average filtering error obtained in the simulations. The small discrepancy between both curves is due to finite sample size effects.

is also a consequence of the Markov nature of the posterior probability. Taking a non-Markov prior process would result in a posterior probability whose parameters could not be described by a set of ordinary differential equations.

In figure 5 we show the comparison between the theoretical result in (20) and simulation results for the prediction error. We can see that the prediction error is very well described by the derived equation.

3. Optimal Population Coding

We can now apply the results from the previous section to study the optimal coding strategies for neurons in the dynamic case. The study of bell-shaped and more specifically Gaussian tuning curves has been frequently discussed in the literature [32, 20, 2, 3]. Our framework treats the case of densely packed Gaussian tuning functions for stochastic dynamic stimuli. We can study the performance of the tuning functions by mapping the minimal mean squared error for an encoder given by a certain tuning

function. In our case, given the sensory neurons, specified by their preferred stimuli Θ_m , the tuning functions are specified by the maximal firing rate ϕ and the tuning width α .

figure 6 shows a colormap of the MMSE for an Ornstein-Uhlenbeck process for a range of values of α and ϕ . There are some clear trends to be observed. First, we note that for any given value of α , increasing the maximal firing rate ϕ leads, not surprisingly, to a decrease in the MMSE. When the value of ϕ tends to zero, the MMSE tends to the equilibrium variance of the observed process, which is expected, as in the absence of spikes, the best estimate of the stimulus is given by the equilibrium distribution of the OU process. A second interesting observation is that for any given fixed value of ϕ there is a finite value of α which minimizes the MMSE. This is in accord with findings in [2, 3, 20], which also report that the optimal tuning width is a finite value, as well as with experimental data [28, 33]. This can be intuitively understood by noting that when we decrease the tuning width keeping ϕ constant, we decrease the population's firing rate λ , and eventually, for very sharp tuning functions, we will have a vanishingly small number of spikes. On the other hand, increasing the width α will lead to a gain in information through more spikes but eventually these spikes become so uninformative that there is no more advantage from increasing α , as these barely give us more information than is already present in the equilibrium distribution. The right panel of figure 6 shows the MMSE as a function of α for some values of ϕ .

The situation is very similar when we consider higher-order processes. Although the decay of the posterior covariance to its equilibrium value follows a more convoluted dynamics, the argument relating α and the improvement in the reconstruction still holds. Figure 7 shows the analog of figure 6 for the process with $P = 2$. We can see that the general structure of the color plot is very similar. One important difference though, is that for the same firing rate, we are able to obtain a larger improvement in the MMSE, relative to the equilibrium variance of the process. This is clear in the right panel of figure 7. This is to be expected, as the higher-order processes have more continuity constraints and are therefore more *predictable*.

3.1. Ecological Analysis of the Optimal Code

We will now look at how the optimal value of α depends on the parameters of the process. We can, fixing ϕ , γ and η find the optimal value of α that minimizes the MMSE. This will give us a mapping of how the optimal tuning width depends on the different parameters of the stimulus. We consider the case of the second-order Ornstein-Uhlenbeck process ($P = 2$). Note that changing γ also influences the signal variance, as the equilibrium variance of the stimulus is given by $\sigma_x^2 = \eta^2/4\gamma^3$. To better separate these influences of the timescale and variance of the stimulus, we chose to look at the process given by an OU process with diffusion coefficient $\eta' = \eta\gamma^{3/2}$ resulting in a equilibrium variance of $\sigma_x^2 = \eta'^2/4$. In that way we can better analyze the influence of the timescale and intensity of the covariance of the stimulus.

This analysis is shown in figure 8 for the second-order OU process. The timescale

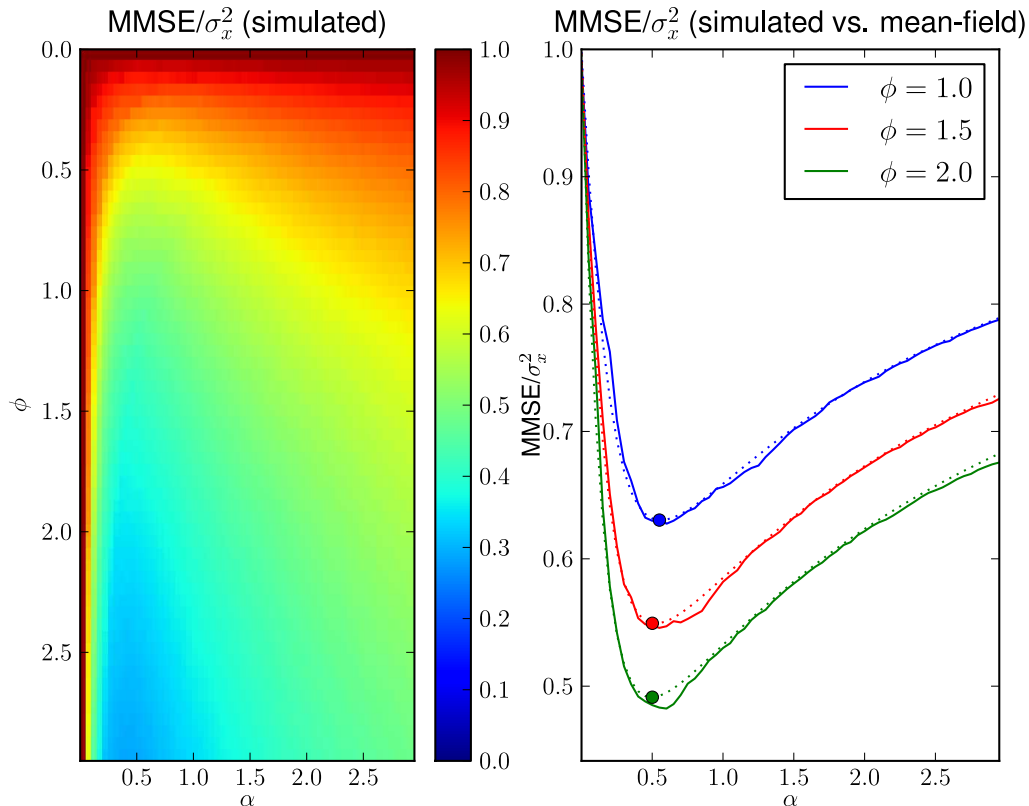


Figure 6: MMSE landscape as a function of the encoder’s tuning width α and maximal firing rate ϕ for the one-dimensional OU process. For simplicity we show the case where $\gamma = \eta = 1$. When either parameters are very near 0, the MMSE is equal to the stimulus’ equilibrium variance. For fixed values of ϕ we observe the existence of a finite optimal tuning width, as is shown in the right panel.

of the process strongly influences the optimal tuning width as can be seen in the figure. With an increase in γ the optimal tuning width increases. This is in accord with the finding in [3], where it was reported that for static stimuli a larger decoding window leads to a narrower optimal tuning width. This can be cast into our framework by making an analogy between the decoding time window and the characteristic time of the decay of the autocorrelation of the observed process. A very large correlation time means a very slowly changing process, which needs less spikes and therefore allows for narrower tuning widths. This can be also understood by referring to the solution for the error distribution of the OU process given by (14). Smaller values of γ allow for a good reconstruction of the stimulus with less spikes. An increase in the stimulus variance σ_x^2 leads to an increase in the optimal tuning width. Meanwhile, an increase in the maximal firing width of each neuron results in a decrease of the optimal tuning width, as is expected. Increasing the height of each tuning function allows the tuning functions to sharpen without decreasing the overall firing rate of the population.

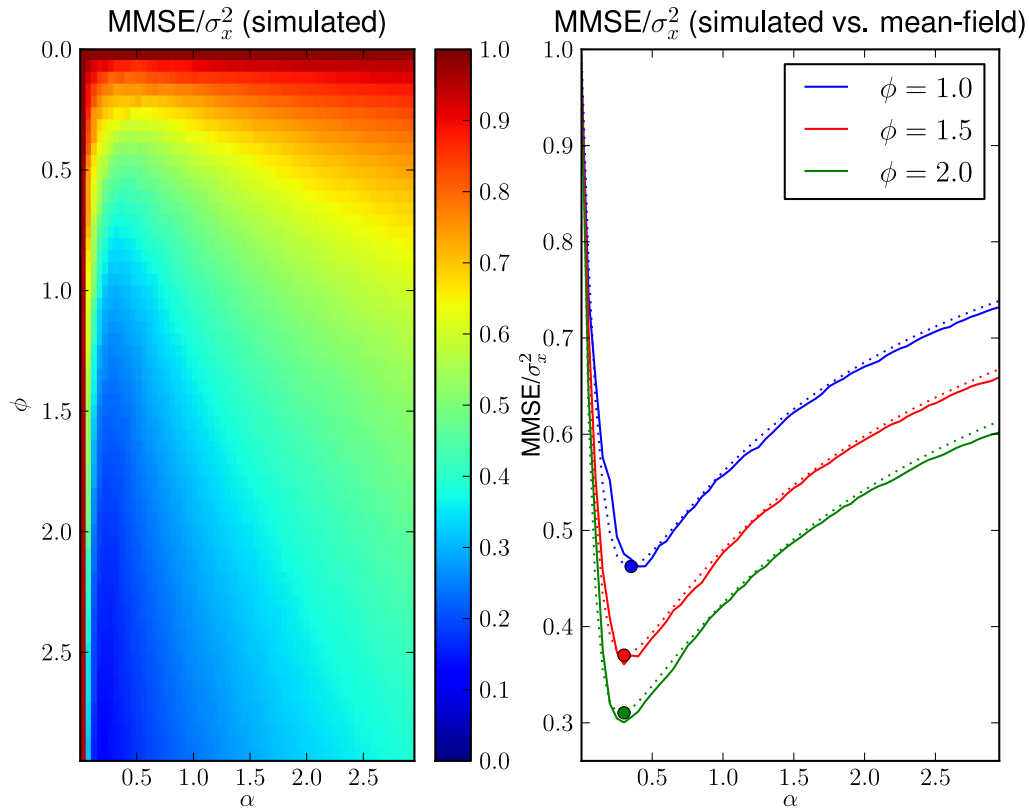


Figure 7: MMSE landscape as a function of the encoder’s tuning width α and maximal firing rate ϕ for the second-order OU process. Again, we show the case where $\gamma = \eta = 1$. When either parameters are very near 0, the MMSE is equal to the stimulus’ equilibrium variance. For fixed values of ϕ we observe the existence of a finite optimal tuning width, as is shown in the right panel.

An interesting perspective on the coding-decoding problem we are studying can be obtained from rate-distortion theory [34], where one seeks the optimal tradeoff between coding rate and reconstruction error (distortion). The celebrated rate-distortion curve provides the smallest rate for which a given level of distortion can be achieved (usually asymptotically). We study the analog of a rate-distortion curve in our case. The rate is given by the average population firing rate λ while the distortion would be the minimal mean squared error. In figure 9 we show a plot of the MMSE of the optimal encoder against the firing rate of the optimal code for given values of ϕ, γ and η . Interestingly, the rate-distortion curve is independent of the value of η . The dependence in γ is as expected. For smaller values of γ (i.e., for longer correlation times), the error decays faster with the population firing rate. Meanwhile, larger values of γ (i.e., shorter correlation times), lead to a slower decay in the distortion as a function of the firing rate.

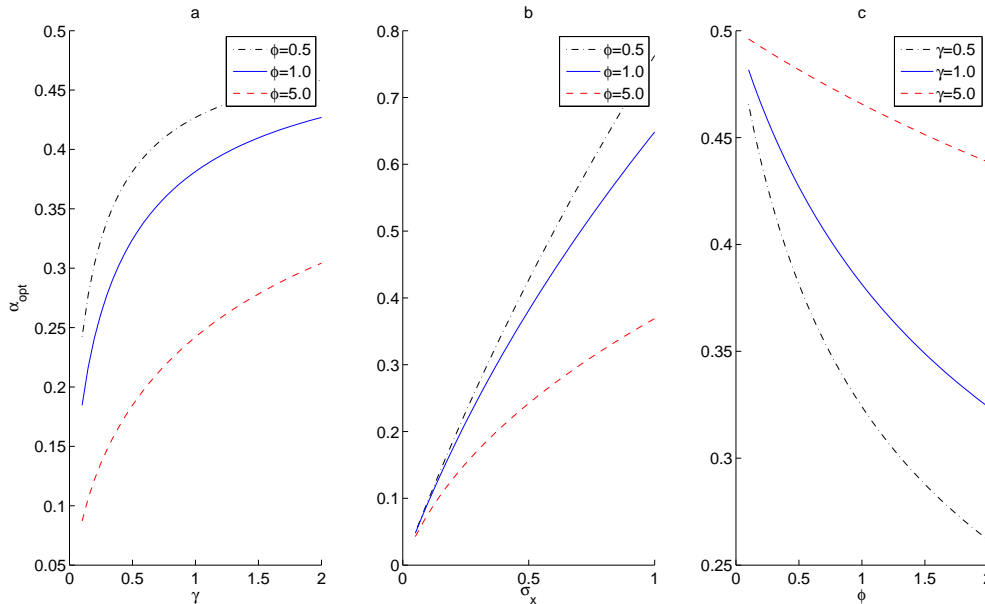


Figure 8: Dependence of the optimal tuning width on the parameters of the stimulus and encoder for the $P = 2$ process. Panel a shows the optimal tuning width as a function of the forcing parameter γ which is the inverse of the characteristic timescale of the stimulus for three different values of the maximal firing rate ϕ . Panel b shows the optimal tuning width as a function of the equilibrium standard deviation of the stimulus for the same values of ϕ . Panel c shows the optimal tuning width as a function of the maximal firing rate of the encoding neurons for three values of the inverse time constant γ .

3.2. Comparison to Previous Research

The existence of an optimal finite tuning width for unimodal tuning curves has been repeatedly determined in the literature. This has been found to be the case with the mutual information as objective function [7] as well as with the reconstruction error as an objective function [20, 3, 2, 35]. Our findings on the optimal tuning width as a function of the correlation time of the observed process, summarized in figure 8, generalize the findings in [3] and in [2] for dynamic processes. Namely, it was established that longer integration times lead to narrower optimal tuning widths. In our case, longer integration times correspond to longer correlation times and therefore smaller values of γ . We have found that for smaller values of γ , i.e. for longer correlation times, the optimal tuning width decreases, as would be expected. Also, as was found in [2], we have established that noisier prior processes lead to broader optimal tuning widths (see figure 8). These results seem to hold in a fairly general set of conditions and this indicates that the tradeoff between firing rate and accuracy is central to the coding strategies in the nervous system.

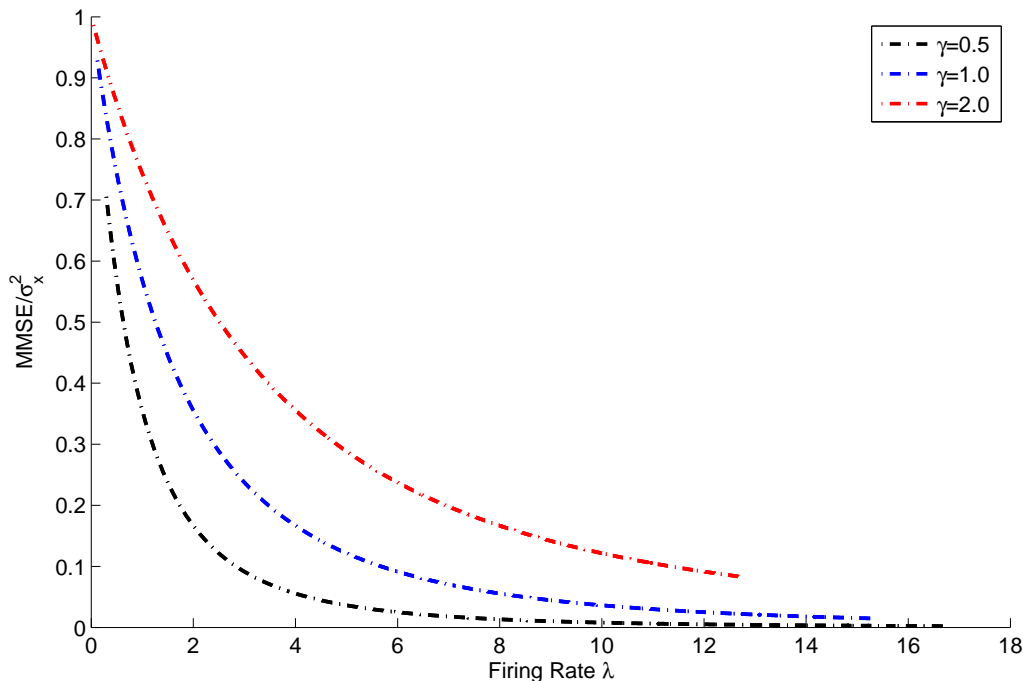


Figure 9: Rate distortion curve of the optimal encoding scheme for the second-order OU process.

4. Discussion

The temporal aspect of neural coding has often been neglected in studies of optimal population coding. A framework for the use of filtering in neural coding had been proposed in [9], but even there the offline paradigm was favored, and most studies either bypass the issue of time completely [4] or resort to time-binning to address the temporal aspects [3, 36]. We have extended the filtering theory presented in [1, 2] for finite-state Markov processes and static processes, where the whole spike train is used for decoding and, using a model of the dynamics of the stimulus, we have addressed the decay of the information as well.

Our framework generalizes a number of findings from previous studies. The finding from [3] and [2] that the reconstruction error decays with the length of the decoding time-window is here framed in terms of the correlation time of the stimulus. We also find the same relation between the optimal tuning width for bell-shaped tuning functions and the correlation time as had been found for the tuning width as a function of the decoding time.

Another advantage of our treatment is that it allows us to study more complex aspects of temporal correlation than just the length of the decoding window. By considering a class of higher-order stochastic processes, we can address different temporal correlation structures. This had been also proposed in [9], but not explored any deeper.

In that spirit, we have established that smoother processes allow for a more efficient coding strategy with the same firing rate in the *sensory* layer. The complexity of the process results in a higher cost in the decoding of the spike train, however, implying that although smooth processes allow for very efficient reconstruction strategies, they will require a more complex decoding strategy. In [37], a decoding strategy using recoding of spikes for RBF processes had been suggested. The approach taken in [1] is to encode the dynamics of the process explicitly into the recurrent connections of the decoding network, which would be straightforward to generalize for smooth processes, but would imply that the number of decoding neurons scales with the order of the process. Clearly, biological systems are not concerned with the degree of continuity, and the model of the temporal structure of the world should be adapted to the (biological and evolutionary) experience of the natural environment. This does, however, suggest a tradeoff between the effort spent in optimally coding a stimulus and the effort spent in decoding it.

Our approach allows for a more flexible and structured way of dealing with the temporal aspects in the neural code. The generalization of the filtering scheme for more complex neuron models such as generalized linear models is relatively simple, although the assumption of dense tuning functions clearly cannot hold then and the solution of the filtering problem will not be Gaussian anymore. One can still consider a Gaussian approximation to it, as has been done in [38], or resort to particle filter approximations [39]. One other interesting direction for further research is to develop filtering approaches to biologically inspired neuron models, such as leaky-integrate-and-fire models. The hurdles in this case are the same, the Gaussian assumption will not hold and we have to work with approximations. However, through a systematic treatment of the resulting problems, more insights might be gained into the temporal aspects of the neural code.

5. Acknowledgements

The work of A.S. was supported by the DFG Research Training Group GRK 1589/1. The work of R.M. was ...

We kindly thank...

6. References

- [1] Omer Bobrowski, Ron Meir, and Yonina C Eldar. Bayesian filtering in spiking neural networks: noise, adaptation, and multisensory integration. *Neural computation*, 21(5):1277–320, May 2009.
- [2] Steve Yaeli and Ron Meir. Error-based analysis of optimal tuning functions explains phenomena observed in sensory neurons. *Frontiers in computational neuroscience*, 4(October):16, 2010.
- [3] Philipp Berens, Alexander S Ecker, Sebastian Gerwinn, Andreas S Tolias, and Matthias Bethge. Reassessing optimal neural population codes with neurometric functions. *Proceedings of the National Academy of Sciences of the United States of America*, 108(11):4423–8, March 2011.
- [4] Gasper Tkacik, Jason S Prentice, Vijay Balasubramanian, and Elad Schneidman. Optimal population coding by noisy spiking neurons. *Proceedings of the National Academy of Sciences of the United States of America*, 107(32):14419–24, August 2010.

- [5] Christian P. Robert. *The Bayesian Choice: From Decision-Theoretical Foundations to Computational Implementation*. Springer, New York, NY, 2nd edition, 2007.
- [6] Donald L Snyder. Filtering and detection for doubly stochastic Poisson processes. *IEEE Transactions on Information Theory*, 18(1):91–102, January 1972.
- [7] Nicolas Brunel and JP Nadal. Mutual information, Fisher information, and population coding. *Neural Computation*, 10(7), 1998.
- [8] Pascal Vincent, Hugo Larochelle, Yoshua Bengio, and Pierre-Antoine Manzagol. Extracting and composing robust features with denoising autoencoders. *Proceedings of the 25th international conference on Machine learning - ICML '08*, pages 1096–1103, 2008.
- [9] Quentin J M Huys, Richard S Zemel, Rama Natarajan, and Peter Dayan. Fast population coding. *Neural Computation*, 19(2):404–441, 2007.
- [10] Claude E. Shannon. The mathematical theory of communication. 1963. *Bell System Technical Journal*, 27:379–423 and 623–656, 1948.
- [11] Aditya Mahajan and Demosthenis Teneketzis. Optimal design of sequential real-time communication systems. *IEEE Transactions on Information Theory*, 55(11):5317–5338, 2009.
- [12] Terrence R Stanford, Swetha Shankar, Dino P Massoglia, M Gabriela Costello, and Emilio Salinas. Perceptual decision making in less than 30 milliseconds. *Nature neuroscience*, 13(3):379–85, March 2010.
- [13] Simon Thorpe, Denis Fize, and Catherine Marlot. Speed of processing in the human visual system. *Nature*, 381(6):520–522, 1996.
- [14] Joseph J Atick. Could information theory provide an ecological theory of sensory processing? *Network: Computation in neural systems*, 3(2):213–251, January 1992.
- [15] Marc O Ernst and Martin S Banks. Humans integrate visual and haptic information in a statistically optimal fashion. *Nature*, 415(6870):429–33, January 2002.
- [16] David C Knill and Alexandre Pouget. The Bayesian brain: the role of uncertainty in neural coding and computation. *Trends in neurosciences*, 27(12):712–9, December 2004.
- [17] Timm Lochmann and Sophie Deneve. Neural processing as causal inference. *Current opinion in neurobiology*, 21(5):774–81, October 2011.
- [18] Martin Boerlin and Sophie Denève. Spike-based population coding and working memory. *PLoS computational biology*, 7(2):e1001080, February 2011.
- [19] Jeffrey Beck, Vikranth R Bejjanki, and Alexandre Pouget. Insights from a simple expression for linear fisher information in a recurrently connected population of spiking neurons. *Neural computation*, 23(6):1484–502, June 2011.
- [20] Matthias Bethge, David Rotermund, and Klaus R Pawelzik. Optimal short-term population coding: When Fisher information fails. *Neural Computation*, 14(10):2317–2351, 2002.
- [21] Brian D O Anderson and John B Moore. *Optimal filtering*, volume 11. Prentice-hall, Englewood Cliffs, NJ, 1979.
- [22] DP Palomar and Sergio Verdú. Representation of mutual information via input estimates. *IEEE Transactions on Information Theory*, 53(2):453–470, 2007.
- [23] N Merhav. Optimum estimation via gradients of partition functions and information measures: a statistical-mechanical perspective. *Information Theory, IEEE Transactions on*, 57(6):3887–3898, 2011.
- [24] Dongning Guo, S Shamai, and Sergio Verdú. Mutual information and conditional mean estimation in Poisson channels. *IEEE Transactions on Information Theory*, 54(5):1837–1849, 2008.
- [25] Rami Atar and Tsachy Weissman. Mutual information, relative entropy, and estimation in the Poisson channel. *2011 IEEE International Symposium on Information Theory Proceedings*, pages 708–712, July 2011.
- [26] Carl Edward Rasmussen and Christopher K. I. Williams. *Gaussian Processes for Machine Learning*. MIT Press, Cambridge, MA, 1st edition, 2005.
- [27] Crispin W Gardiner. *Handbook of Stochastic Methods: for Physics, Chemistry and the Natural Sciences*, volume Vol. 13 of *Series in synergetics*. Springer, 2004.

- [28] Andrea Benucci, Dario L Ringach, and Matteo Carandini. Coding of stimulus sequences by population responses in visual cortex. *Nature neuroscience*, 12(10):1317–24, October 2009.
- [29] John O’Keefe and Jonathan Dostrovsky. The hippocampus as a spatial map . Preliminary evidence from unit activity in the freely-moving rat. *Brain Research*, 34:171–175, 1971.
- [30] James J Knierim, Hemant S Kudrimoti, and Bruce L McNaughton. Place cells, head direction cells, and the learning of landmark stability. *The Journal of Neuroscience*, 15(3):1648–1659, 1995.
- [31] Donald L Snyder and Michael I Miller. *Random Point Processes in Time and Space*. Springer-Verlag, 1991.
- [32] Kechen Zhang and TJ Terrence J. Sejnowski. Neuronal tuning: To sharpen or broaden? *Neural Computation*, 11(1):75–84, 1999.
- [33] Yoram Gutfreund and Eric I Knudsen. Adaptation in the auditory space map of the barn owl. *Journal of Neurophysiology*, 96(2):813–25, 2006.
- [34] Thomas M Cover and Joy A Thomas. *Elements of Information Theory*, volume 6 of *Wiley Series in Telecommunications*. Wiley, 1991.
- [35] Alex Susemihl, Ron Meir, and Manfred Oppel. Analytical Results for the Error in Filtering of Gaussian Processes. In J. Shawe-Taylor, R. S. Zemel, P. Bartlett, F.C.N. Pereira, and K.Q. Weinberger, editors, *Advances in Neural Information Processing Systems*, pages 2303–2311, 2011.
- [36] Sebastian Gerwinn, Jakob Macke, and Matthias Bethge. Bayesian Population Decoding of Spiking Neurons. *Frontiers in computational neuroscience*, 3(October):14, 2009.
- [37] Rama Natarajan, Quentin J M QJM Huys, Peter Dayan, and Richard S RS Zemel. Encoding and Decoding Spikes for Dynamic Stimuli. *Neural computation*, 20(9):1–36, 2008.
- [38] Jean-Pascal Pfister, Peter Dayan, and Máté Lengyel. Synapses with short-term plasticity are optimal estimators of presynaptic membrane potentials. *Nature neuroscience*, 13(10):1271–5, October 2010.
- [39] Dan Crisan and Boris Rozovskii. *The Oxford Handbook of Nonlinear Filtering*. Oxford University Press, Oxford, 2011.

Appendix A. Definition of Γ and H

To obtain the process defined in (1) we define

$$\Gamma_{i,j} = -\delta_{i+1,j} + \delta_{P,i} \binom{P}{j-1} \gamma^{P-j+1}, \text{ and } H_{i,j} = \delta_{i,P} \delta_{j,P} \eta.$$

Appendix B. Definition of the Pseudo-determinant

The pseudo-determinant of a square $n \times n$ matrix A is given by

$$\det^*(A) = \lim_{\alpha \rightarrow 0} \frac{\det(A + \alpha I)}{\alpha^{n - \text{rank}(A)}}.$$

For positive semi-definite matrices as are used in the text, the pseudo-determinant is the product of all non-zero eigenvalues.

Appendix C. Boundary Conditions for the Differential Chapman-Kolmogorov Equation

We want to show that in the equilibrium $P(s)_{eq} = 0, \forall s > \eta^2/2s$. We will proceed by cases. If $\alpha^2 < \eta^2/2\gamma$, we have that the jump term will be absent of (11) for $s > \eta^2/2s$ and we will have

$$\frac{\partial P(s, t)}{\partial t} = \frac{\partial}{\partial s} ((2\gamma s - \eta^2)P(s, t)) - \lambda P(s, t).$$

It is easy to see that given a solution of equation

$$\frac{\partial P^*(s, t)}{\partial t} = \frac{\partial}{\partial s} ((2\gamma s - \eta^2)P^*(s, t))$$

with some initial condition $P^*(s, t_0) = P_0(s)$, $P(s, t) = e^{-\lambda(t-t_0)}P^*(s, t)$ is a solution of the first equation with the same initial condition. Therefore $P(s, t) < P^*(s, t)$, $t > t_0$. But $P^*(s, t)$ is the solution of the Liouville equation for the system $\dot{s} = -2\gamma s + \eta^2$. Namely, as $t \rightarrow \infty$, $P^*(s, t) \rightarrow \delta(s - \eta^2/2\gamma)$. Therefore, $\forall s > \eta^2/2\gamma$, $P(s, t) \rightarrow 0$, as $t \rightarrow \infty$.

If $\alpha^2 > \eta^2/2\gamma$, we first proceed in the same manner, but taking $s > \alpha^2$ and imposing an absorbing boundary condition at $s = \alpha^2$. Thus we show that $P(s, t)_{eq} = 0, \forall s > \alpha^2$. We can then subsequently apply the same argument for the intervals $[j^n(\alpha^2), j^{n-1}(\alpha^2)]$, as long as $j^n(\alpha^2) > \eta^2/2\gamma$. Finally, we use the same argument for $[\eta^2/2\gamma, j^m(\alpha^2)]$, where m is the highest integer such that $j^m(\alpha^2) > \eta^2/2\gamma$. This shows our desired result.